ELSEVIER

Journal of Chromatography A, 678 (1994) 85–96

JOURNAL OF CHROMATOGRAPHY A

Velocity profiles in thermal field-flow fractionation

Jamel Eddine Belgaied, Mauricio Hoyos, Michel Martin*

École Supérieure de Physique et Chimie Industrielles, Laboratoire de Physique et Mécanique des Milieux Hétérogènes (URA CNRS 857), 10 Rue Vauquelin, 75231 Paris Cedex 05, France

(First received February 18th, 1994; revised manuscript received April 27th, 1994)

Abstract

Exact velocity profiles in thermal field-flow fractionation (FFF) were numerically computed for twelve solvents and forty different combinations of the temperature drop ΔT across the channel and of the cold wall temperature, T_c. An expression with six coefficients relating the ν parameter of a third-degree polynomial velocity profile which approximates the exact profile with ΔT and T_c was derived for each solvent. Under typical experimental conditions, it provides a nearly two orders of magnitude improvement in the accuracy of the prediction of the retention over the equation based on the classical parabolic profile. A procedure is suggested for using this ν vs. ΔT and T_c expression for extracting the basic FFF parameter λ from retention data.

1. Introduction

Field-flow fractionation (FFF) is a method of separation of macromolecular or particulate materials which is performed in a thin, ribbon-like channel. A flow of carrier liquid transports the sample components along the channel at various rates depending on their degree of interaction with an external field applied perpendicular to the main axis of the channel [1]. The retention time of a sample component (which, in the following, will be called an analyte) depends on both its concentration distribution and the axial velocity distribution in the field direction. Therefore, in order to predict the retention of an analyte or to characterize an analyte from its FFF retention data, one needs to know these two distributions precisely. The concentration distribution depends on the forces acting on the analyte and on its diffusivity. In fact, the shape of this distribution determines the operating retention mode [2].

Because the analytes generally have a small size, it can be correctly assumed in most cases, that they are transported along the channel by the flow with the axial flow velocity at the position of their centre of gravity. Knowing the axial velocity distribution of the analytes in the field direction then amounts to knowing the axial flow profile. Because the channel is essentially made of two long and wide parallel walls, the flow profile is frequently assumed to be parabolic, except for a small perturbation near the channel edges [3,4]. Such a velocity profile is obtained for the flow of an isothermal fluid between two infinite parallel plates. Indeed, if z is the direction of the flow, x the distance from one of the plates, w the distance between the

* Corresponding author.

0021-9673/94/$07.00
SSDI 0021-9673(94)00419-A

two plates, dP/dz the pressure gradient driving the flow and η the fluid viscosity, the velocity profile, $v(x)$, is then obtained from the simple form of the differential Navier–Stokes equation:

$$\eta \cdot \frac{d^2v}{dx^2} = \frac{dP}{dz} \tag{1}$$

which gives, after integration:

$$\frac{v(x)}{\langle v \rangle} = 6\left[\left(\frac{x}{w}\right) - \left(\frac{x}{w}\right)^2\right] \tag{2}$$

where $\langle v \rangle$ is the mean flow velocity. There are, however, situations encountered in FFF where these two underlying assumptions (infinite parallel plates geometry and constant viscosity) are not fulfilled. Such is the case, for instance, in sedimentation FFF because of the curved geometry of the channel, or in flow FFF because of a transverse flow component through at least one of the channel walls. Nevertheless, under typical operating conditions, the correction to be brought to the flow profile is then negligibly small [2].

The situation is clearly different in thermal FFF in which the variations of the fluid viscosity resulting from the temperature gradient applied across the channel thickness are sufficiently large to induce significant distortion of the flow profile from the parabolic limit. This was recognized in earlier papers on thermal FFF. Myers et al. [5] solved Eq. 1 in which η is no longer a constant but is given as a function of x as

$$\eta = \eta_c \exp(-\beta x/w) \tag{3}$$

where $\beta = B\,\Delta T/T_c^2$, η_c is the viscosity at temperature T_c of the cold wall, ΔT is the temperature difference between the two plates and B a solvent constant in the Andrade equation relating the viscosity and the absolute temperature T:

$$\eta = \eta_c \exp\left[B\left(\frac{1}{T} - \frac{1}{T_c}\right)\right] \tag{4}$$

Comparison of Eqs. 3 and 4 shows that the following relationship was implicitly assumed for the temperature profile across the channel thickness:

$$T = \frac{T_c}{1 - \dfrac{\Delta T}{T_c} \cdot \dfrac{x}{w}} \tag{5}$$

this equation may provide a satisfactory approximation of the temperature profile near the cold wall but is not consistent with the fact that ΔT represents the temperature drop between the two plates.

It was later pointed out that, when the viscosity is not constant, the left-hand term of Eq. 1 is not correct, even when taking η as a function of x, but must also include a $d\eta/dx$ term [6]. The flow profile was accordingly calculated using Eq. (4) and a linear relationship between T and x [7]. However, the calculation is complex and has to be made numerically for specific values of B, T_c and ΔT, as some of the integrals involved have no analytical solution.

Further, the temperature profile across the channel thickness is actually not linear because of the temperature dependence of the thermal conductivity of the liquid. Knowing this dependence, one can calculate the resulting temperature profile [8]. This further complicates the calculation of the velocity profile. A treatment was performed by Gunderson et al. [9] using the complete Navier–Stokes equation, a third-degree polynomial expression of the fluidity, which is the reciprocal of the viscosity, as a function of the temperature and a third-degree polynomial dependence of the temperature vs. x/w, obtained as a Taylor series about the cold wall in terms of $d\kappa/dT$, the coefficient of variation of the thermal conductivity κ with temperature. By this means, they were able to obtain an analytical solution of the velocity profile given as a fifth-degree polynomial expression in terms of the reduced coordinate x/w. Then the retention equation, for an exponential concentration profile, was obtained as a particular case of the general expression for a n-degree polynomial velocity profile given previously [10].

In spite of the fact that analytical expressions of the velocity profile and of the retention factor are obtained, this procedure is sometimes considered complicated because various successive calculations must be performed to obtain the coefficients of the velocity profile expression

[11]. In addition, the Taylor expansion of the temperature profile about the cold wall cannot rigorously provide the correct value of the temperature at the hot wall and is therefore not, in principle, rigorously consistent with the fact that the temperature drop between the two plates is equal to ΔT. Further, the computation of the dispersion coefficients for a fifth-degree polynomial velocity profile becomes very complex and has not yet been attempted, although general expressions for an n-degree polynomial velocity profile exist [10].

For this reason, it has been suggested that one can approximate the true velocity profile by a third-degree polynomial profile in such a way that the slope of the relative velocity profile becomes equal to that of the true profile as one approaches the cold wall [10,12,13]. This method is justified by the fact that it has been observed that all investigated polymeric samples analysed so far using thermal FFF move in the vicinity of the cold wall where they form a thin cloud. This method has been applied in some instances for predicting or interpreting retention data [12–16]. A third-degree polynomial velocity profile contains a single adjustable coefficient as the three other possible coefficients of a third-degree polynomial are fixed by the no-slip condition (which implies a zero velocity at each of the two walls) and the normalization condition (the mean value of the relative profile $v/\langle v\rangle$ across the thickness must be equal to 1). The main problem is selecting the appropriate third-degree coefficient for specific solvent and temperature conditions. This has mainly been done by graphical interpolation of calculations at various B/T_c and $\Delta T/T_c$ values [17]. The purpose of this work was to provide a method for calculating the third-degree coefficient for various solvents and temperature conditions, which can be easily used for practical application in both predicting and interpreting thermal FFF retention data.

2. Theory

The basic Navier–Stokes equation describing the flow velocity in the case of a non-constant viscosity is written as [6,18,19]

$$\frac{\mathrm{d}}{\mathrm{d}x}\left(\eta\frac{\mathrm{d}v}{\mathrm{d}x}\right)=\eta\frac{\mathrm{d}^2v}{\mathrm{d}x^2}+\frac{\mathrm{d}\eta}{\mathrm{d}x}\cdot\frac{\mathrm{d}v}{\mathrm{d}x}=\frac{\mathrm{d}P}{\mathrm{d}z} \tag{6}$$

By double integration of this equation, the relative velocity profile, $v/\langle v\rangle$, is obtained as a function of the reduced transverse coordinate, x/w:

$$\frac{v}{\langle v\rangle}=\frac{\int_0^{x/w}\frac{x/w}{\eta}\,\mathrm{d}(x/w)-C\int_0^{x/w}\frac{\mathrm{d}(x/w)}{\eta}}{\int_0^1\left(\int_0^{x/w}\frac{x/w}{\eta}\,\mathrm{d}(x/w)-C\int_0^{x/w}\frac{\mathrm{d}(x/w)}{\eta}\right)\mathrm{d}(x/w)} \tag{7}$$

where η depends on x/w through the temperature T. The constant C in Eq. 7 is equal to

$$C=\frac{\int_0^1\frac{x/w}{\eta}\,\mathrm{d}(x/w)}{\int_0^1\frac{\mathrm{d}(x/w)}{\eta}} \tag{8}$$

The relationship between the viscosity and the temperature used in this work is given by Eq. (4). This form of the Andrade equation is consistent with experimental data [20] and with approximate theories of the liquid state [21]. Considering Eq. 4 as an Arrhenius-type law, kB, where k is the Boltzmann constant, can be considered as an activation energy for viscous flow.

The thermal FFF system is generally operated in such a way that a constant energy flux, q, is input to the channel by means of electrical resistances in the vicinity of the hot wall, while a flow of water evacuates the heat at the cold wall. The temperature profile across the channel thickness is then given by the Fourier law of heat conduction [22]:

$$q=-\kappa\cdot\frac{\mathrm{d}T}{\mathrm{d}x} \tag{9}$$

where κ is the thermal conductivity. Over the typical temperature ranges encountered in ther-

mal FFF experiments, the thermal conductivity changes slightly and linearly with temperature [23] so that one can write

$$\kappa = \kappa_c + \frac{d\kappa}{dT}(T - T_c) \tag{10}$$

where κ_c is the thermal conductivity at the cold wall temperature and $d\kappa/dT$ is a constant specific for the carrier liquid. Integration of Eq. 9 in combination with Eq. 10 and elimination of q by replacement in terms of ΔT, the temperature drop between the two plates, gives the temperature profile across the channel thickness [9]:

$$T = T_c + \frac{1}{\frac{1}{\kappa_c}\cdot\frac{d\kappa}{dT}} \times \left(\sqrt{1 + \frac{2}{\kappa_c}\cdot\frac{d\kappa}{dT}\cdot\Delta T\left(1 + \frac{1}{\kappa_c}\cdot\frac{d\kappa}{dT}\cdot\frac{\Delta T}{2}\right)\frac{x}{w}} - 1\right) \tag{11}$$

Replacement of T in Eq. 4 by its expression in Eq. 11 provides the dependence of η as a function of x/w which is needed for evaluating the integrals which gives the velocity profile in Eq. 7 for given B, T_c, η_c, ΔT, κ_c and $d\kappa/dT$ values. As B, η_c, κ_c and $d\kappa/dT$ depend on the nature of the carrier liquid and on T_c, the three independent parameters which determine the velocity profile are ΔT, T_c and the nature of the carrier liquid. The relative velocity profiles were numerically calculated according to Eqs. 7, 4 and 11 for various liquids, ΔT and T_c values. They are referred to as "exact" velocity profiles, $(v/\langle v\rangle)_{ex}$.

As discussed above, it is interesting, from a practical point of view, to approximate the exact relative velocity profile by a third-degree polynomial profile, $(v/\langle v\rangle)_3$, in terms of x/w. It has been found convenient to write this profile, which depends on the single adjustable coefficient ν, in such a way that one retrieves the parabolic profile when $\nu = 0$ [10,13]. This gives

$$\left(\frac{v}{\langle v\rangle}\right)_3 = 6\left[(1+\nu)\left(\frac{x}{w}\right) - (1+3\nu)\left(\frac{x}{w}\right)^2 + 2\nu\left(\frac{x}{w}\right)^3\right] \tag{12}$$

In order to select ν so that the slope of the exact relative velocity profile equals that of the third-degree profile near the cold wall, the procedure developed by Brimhall et al. [7] cannot be employed as it is specific for a linear temperature profile. We therefore use the following general approach.

One can compare a given relative velocity profile with the ideal parabolic shape, $(v/\langle v\rangle)_2$, given by Eq. 2 and obtained for $\Delta T = 0$ or for a hypothetical liquid with $B = 0$, by means of the relative deviation, ε, defined as

$$\varepsilon = \frac{(v/\langle v\rangle) - (v/\langle v\rangle)_2}{(v/\langle v\rangle)_2} \tag{13}$$

This relative deviation depends, of course, on x/w. In fact, a plot of ε vs. x/w can be considered as a modified representation of a velocity profile. Let ε_{ex} and ε_3 be the ε functions for the exact and third-degree polynomial velocity profiles, respectively. The slope of the exact relative velocity profile is, according to Eq. 13, equal to

$$\frac{d(v/\langle v\rangle)_{ex}}{d(x/w)} = (1+\varepsilon_{ex})\frac{d(v/\langle v\rangle)_2}{d(x/w)} + (v/\langle v\rangle)_2\frac{d\varepsilon_{ex}}{d(x/w)} \tag{14}$$

It is easily seen from Eq. 12 that the slope of the third-degree relative velocity profile at cold wall is equal to $6(1+\nu)$. In order to approximate the exact velocity profile by a third-degree polynomial velocity profile in such a way that the two profiles have the same slope at the cold wall, one therefore must have

$$\left.\frac{d(v/\langle v\rangle)_{ex}}{d(x/w)}\right|_{x/w=0} = 6(1+\nu) \tag{15}$$

Noting that, at the cold wall $(x/w = 0)$, $(v/\langle v\rangle)_2 = 0$ and $d(v/\langle v\rangle)_2/d(x/w) = 6$ according to Eq. 2, the combination of Eqs. 14 and 15 gives

$$\lim_{x/w\to 0}\varepsilon_{ex} = \nu \tag{16}$$

One notes that, according to Eq. 12, ε becomes undefined for vanishing x/w, so one has then to write ε_{ex} as a limit. The physical property of the

parameter ν expressed by eqn. 16 provides an easy graphical representation of the ν parameter: this is the limiting value of ε_{ex} for $x/w = 0$. This property is used in the following for the determination of ν.

Assuming that the concentration profile of a given solute is exponential and characterized by the basic FFF parameter, λ, of that solute, its retention factor, R, is then obtained, when the velocity profile is represented by Eq. 12, in terms of λ and ν as [10,13]

$$R = 6\lambda\left\{\nu + (1 - 6\lambda\nu)\left[\coth\left(\frac{1}{2\lambda}\right) - 2\lambda\right]\right\} \qquad (17)$$

3. Basic solvent data and computational procedure

The computation of the relative velocity profile for a given solvent at various T_c and ΔT values requires that the values of the constants B and $d\kappa/dT$ of that solvent and the value of κ at some reference temperature are known. The values of B for the various organic solvents were calculated as the slopes of the linear regressions of $\ln \eta$ vs. $1/T$ from experimental viscosity data at various temperatures [20,24]. The resulting B values for the various solvents investigated are reported in Table 1.

When experimental thermal conductivity data for a given solvent were reported at different temperatures [23], $d\kappa/dT$ was calculated as the slope of a linear regression of κ vs. T. In other cases, values of κ were estimated at various temperatures using the Latini et al. method recommended for organic solvents by Reid et al. [23], which gives

$$\kappa = \frac{A^* T_b^{\alpha}}{M^{\beta} T_{crit}^{\gamma}} \cdot \frac{(1 - T_r)^{0.38}}{T_r^{1/6}} \qquad (18)$$

where T_r is the reduced temperature T/T_{crit}, T_{crit} the critical temperature, T_b the normal boiling temperature, M the solvent molecular mass and A^*, α, β, γ parameters which are tabulated for various classes of organic compounds [23]. Although this expression is not rigorously consistent with the hypothesis of the constancy of $d\kappa/dT$, it is found that the variation of κ with T in the typical temperature range used in FFF is nearly linear, which justifies the approximation expressed by Eq. 10. The values of κ at 20°C and of $d\kappa/dT$ are reported in Table 1.

Once the viscosity profile, $\eta(x/w)$, across the channel thickness is known from the combination of Eqs. 4 and 11 for a given solvent and fixed values of T_c and ΔT, the integrals entering Eqs. 7 and 8 are numerically computed by means

Table 1
Solvent properties used in the calculations

Solvent	B (K)	κ at 293 K ($Wm^{-1}K^{-1}$)	$d\kappa/dT$ ($Wm^{-1}K^{-2}$)
Benzene	1315.79	0.148	$-3.53 \cdot 10^{-4}$
2-Butanone	975.90	0.160[a]	$-2.80 \cdot 10^{-4}$[a]
Carbon tetrachloride	1242.32	0.103	$-1.87 \cdot 10^{-4}$[a]
Cyclohexane	1516.57	0.124	$-2.48 \cdot 10^{-4}$[a]
Cyclohexanone	1791.00	0.170[a]	$-2.86 \cdot 10^{-4}$[a]
p-Dioxane	1311.17	0.159[a]	$-2.95 \cdot 10^{-4}$[a]
Ethyl acetate	1042.33	0.147	$-1.50 \cdot 10^{-4}$
Ethylbenzene	1095.78	0.132	$-2.33 \cdot 10^{-4}$
Tetrahydrofuran	923.21	0.166[a]	$-3.51 \cdot 10^{-4}$[a]
Toluene	1085.00	0.141[a]	$-2.59 \cdot 10^{-4}$[a]
o-Xylene	1183.00	0.139[a]	$-2.11 \cdot 10^{-4}$[a]
p-Xylene	1052.24	0.136[a]	$-2.35 \cdot 10^{-4}$[a]

[a] Values estimates by the Latini et al. method [23].

of the Simpson integration procedure. The relative velocity profile is determined for successive x/w values differing by 0.01 unit. Between two consecutive x/w values, the integrals are computed by dividing the 0.01 interval for x/w in as many sub-intervals as necessary to ensure that the results of the integration of two consecutive two fold division steps differ in relative value by less than 10^{-5}. This integration procedure was tested with some usual functions for which the analytical solution of the finite integral is known. In all cases, the relative difference between the numerical and analytical integration results was less than $5 \cdot 10^{-7}$.

Then, knowing the exact relative velocity profile, the relative deviation, ε_{ex}, from the parabolic profile is calculated and the ν parameter is estimated according to the property expressed by Eq. 16, by extrapolation to $x/w = 0$ of the ε_{ex} vs. x/w curve for small x/w values. In practice, ν is obtained as the intercept of the linear regression of ε_{ex} vs. x/w in the x/w range from 0.01 to 0.1.

4. Results and discussion

The temperature profile given by Eq. 11 is represented in Fig. 1 together with two approximate profiles previously used, the linear profile [7] and the profile given by Eq. 5 [5]. Clearly, this latter profile does not describe the true profile satisfactorily. The deviation of this true profile from linearity depends on ΔT, on the solvent used and, to a lesser extent, on T_c. Since for all organic solvents investigated the thermal conductivity decreases with increasing temperature, the shape of the temperature profile is similar to that shown in Fig. 1 and at any position across the channel the actual temperature is lower than it would be if the profile was linear.

The relative velocity profiles and the associated ν parameters were determined for the twelve organic solvents listed in Table 1, which have been or may be used in thermal FFF. For each solvent, 40 sets of calculations were performed for four T_c values ($T_c = 10$, 20, 30 and 40°C) and ten ΔT values ($\Delta T = 10$, 20, 30, 40, 50, 60, 70, 80, 90 and 100°C).

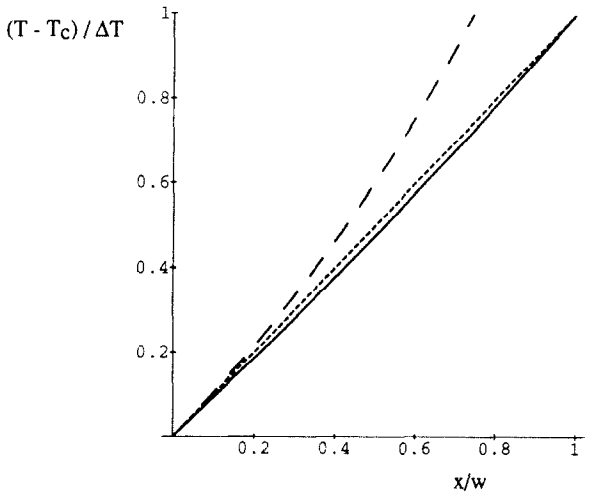

Fig. 1. Temperature profiles in thermal FFF plotted as $(T - T_c)/\Delta T$ vs. x/w. From bottom to top curves: exact profile with temperature-dependent thermal conductivity; linear profile (temperature-independent thermal conductivity); profile given by Eq. 5. Solvent, ethylbenzene; $\Delta T = 100$°C; $T_c = 20$°C.

For all solvents except two (cyclohexanone and *o*-xylene), the overall temperature range covered from the lowest cold wall temperature (10°C) to the highest hot wall temperature (140°C) exceeds the liquid temperature range at atmospheric pressure. When performing the calculations it was implicitly assumed that the values of the solvent parameters B, κ_c and $d\kappa/dT$ obtained or estimated at atmospheric pressure were also correct at the pressure necessary to maintain the carrier fluid in the liquid state at the hot wall temperature selected. In fact, it is relatively rare that thermal FFF experiments are performed in a pressurized channel. Exceptions concern the analysis of relatively low-molecular mass species for which a large ΔT is necessary to obtain the required selectivity [25], the analysis of polymers, such as polyethylenes, for which a high T_c is needed to satisfy the solubility requirement [26] or, still, the case of solvents with low boiling points. Therefore, even if pressure effects on viscosity and thermal conductivity are significant, the above assumption remains applicable to

derive trends in the variations of ν when changing ΔT and/or T_c at atmospheric pressure, which is done below.

A typical velocity profile is shown in Fig. 2 together with the corresponding third-degree polynomial profile and the ideal parabolic profile. Obviously, as follows from the definition of ν, the exact and third-degree profiles become identical as one approaches the cold wall ($x/w = 0$). They are close to each other but differ significantly from the parabolic profile. The position of the maximum velocity appears to be shifted from the channel centre ($x/w = 0.5$) towards the hot wall. It can be shown that, for the third-degree polynomial velocity profile, this position is given by

$$(x/w)_{max} = \frac{1 + 3\nu - \sqrt{1 + 3\nu^2}}{6\nu} \quad (19)$$

The maximum relative velocity, which is equal to

$$\frac{v_{max}}{\langle v \rangle} = -\frac{1}{9\nu^2}[1 - 9\nu^2 - (1 + 3\nu^2)\sqrt{1 + 3\nu^2}] \quad (20)$$

is slightly larger than for the parabolic profile. For instance, for $\nu = -0.2$, one obtains $(x/w)_{max} = 0.549$ and $v_{max}/\langle v \rangle = 1.515$.

The relative deviations of the exact and corresponding third-degree polynomial velocity profiles from the parabolic profile are more easily observed in the plots of ε_{ex} and ε_3, respectively, vs. x/w as seen in Fig. 3. In this kind of ε vs. x/w plot, the parabolic profile is simply represented as the straight horizontal line $\varepsilon = 0$ for all x/w. It is easily seen from Eq. 12 that the relative deviation, ε_3, for a third-degree velocity profile is a straight line with a slope equal to -2ν and passing through the point $[\varepsilon_3 = 0, x/w = 1/2]$:

$$\varepsilon_3 = \nu\left(1 - 2 \cdot \frac{x}{w}\right) \quad (21)$$

The exact relative velocity profile has, in the ε vs. x/w representation, a more complex shape as seen in Fig. 3. As mentioned in the theoretical section, the ν parameter is given as the value of the limiting value of ε_{ex} when one approaches $x/w = 0$. As the viscosity decreases with increasing temperature, the velocity in the vicinity of the cold wall is lower than it would be if the profile was parabolic. Therefore, the ν parameters in thermal FFF are negative as long as the cold wall is the accumulation wall. In the case of ethylbenzene with $\Delta T = 100°C$ and $T_c = 20°C$ corresponding to the curves in Fig. 3, one has $\nu = -0.2922$. This value is large and shows that the temperature effect on the velocity profile must be taken into account when interpreting retention data in thermal FFF. Indeed, neglecting this effect by using the classical retention

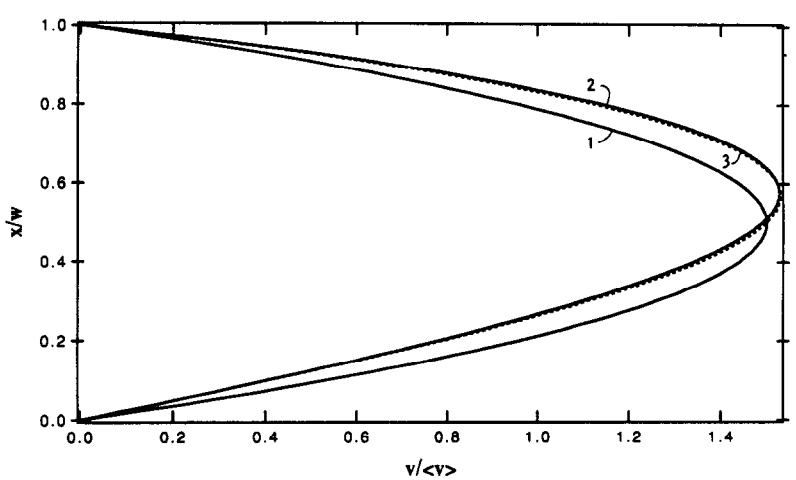

Fig. 2. Relative velocity profiles plotted as x/w vs. $v/\langle v \rangle$. 1 = parabolic profile; 2 = exact profile; 3 = third-degree polynomial profile. Solvent, ethylbenzene; $\Delta T = 100°C$; $T_c = 20°C$.

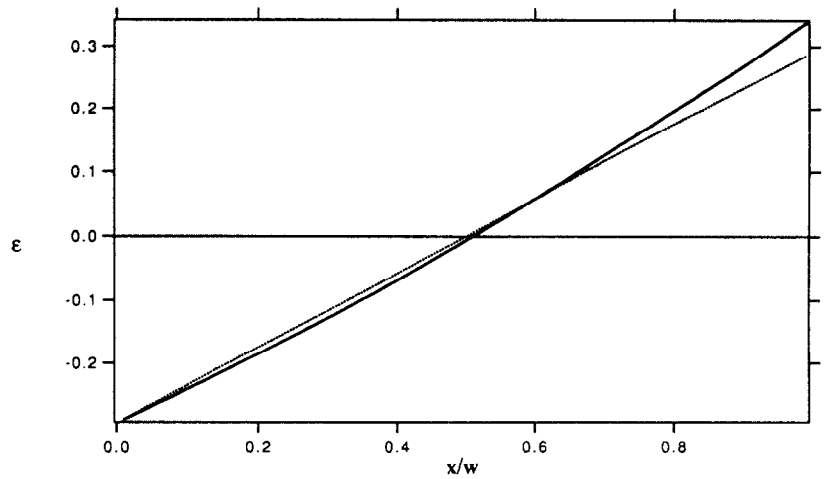

Fig. 3. Relative deviation, ε, of the exact relative velocity profile from the parabolic profile vs. x/w (solid curve). The straight line (dotted line) represents the relative deviation of the corresponding third-degree polynomial velocity profile from the parabolic profile. The ν parameter is given as the intercept of this straight line (in this case $\nu = -0.29218$). Solvent, ethylbenzene; $\Delta T = 100°C$; $T_c = 20°C$.

equation for a parabolic profile will, in the high retention domain, result in a nearly 29% error in the basic FFF parameter λ, which, in turn, will correspond to a 87% error in the determination of the molecular mass of a polystyrene sample from a known relationship between λ and molecular mass.

The deviation of the velocity profile from the parabolic shape arises from the temperature dependence of the carrier liquid viscosity. However, the influence of this effect depends on the temperature profile. The influence of the variation of the thermal conductivity with temperature has only a minor effect on the resulting velocity profile. Indeed, it can be shown that, for ethylbenzene with $T_c = 20°C$, in the relatively extreme case where $\Delta T = 100°C$, the exact relative velocity profile and the relative velocity profile that would be obtained if the thermal conductivity was independent of the temperature are very close to each other. Their maximum values differ by less than 0.2%. The corresponding ν parameters are equal to -0.2922 and -0.2999, respectively.

The dependence of ν with ΔT is plotted for ethylbenzene in Fig. 4a at various T_c values; ν, which reflects the distortion of the flow profile from the parabolic shape, is seen to increase in absolute value with increasing ΔT. For a given ΔT, $|\nu|$ increases with decreasing T_c. A three-dimensional representation of ν vs. ΔT and T_c is shown for ethylbenzene in Fig. 4b. Similar curves are obtained for other organic solvents listed in Table 1.

In order to allow an easy determination the ν parameter corresponding to the solvent and temperature conditions of a given thermal FFF experiment without performing the lengthy calculations involved in the procedure described above, the set of 40 ν values obtained for a given solvent served as a database for finding a correlation for ν as a function of ΔT and T_c. Because the variation of ν with T_c at a given ΔT is nearly linear and that with ΔT at a given T_c is nearly quadratic, the following regression was tested by means of the least-mean square method:

$$\nu = (a_1 T_c + a_2)\,\Delta T + (a_3 T_c + a_4)\,\Delta T^2 + (a_5 T_c + a_6)\,\Delta T^3 \quad (22)$$

The fit is satisfactory for the twelve solvents. The relative error in ν arising from the regression was determined by comparing values given by Eq. 22 with the original ν values. It is found to be lower

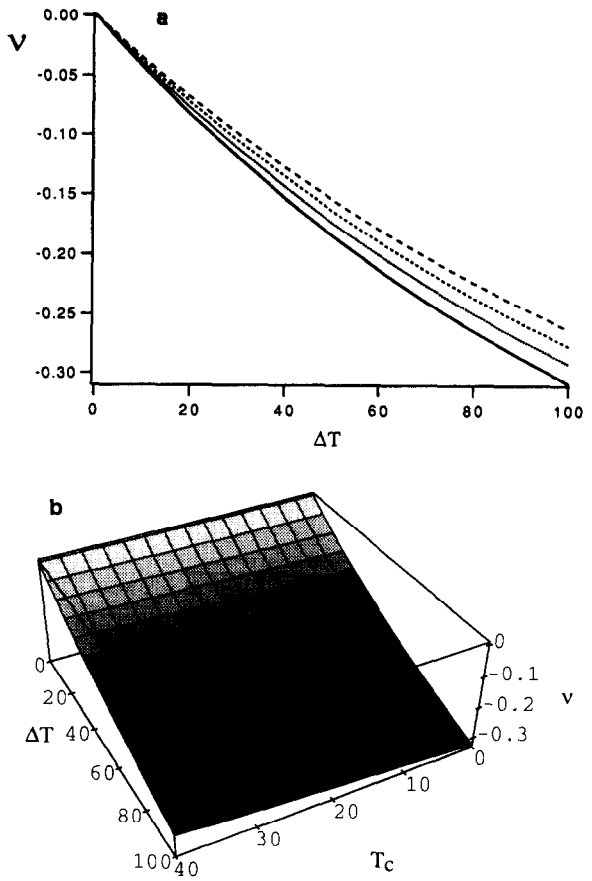

Fig. 4. Variations of the ν parameter with ΔT and T_c. (a) ν vs. ΔT at $T_c = 10$, 20, 30 and 40°C from bottom to top curve; (b) three-dimensional representation of ν vs. ΔT and T_c. Solvent, ethylbenzene.

than 0.4% in all instances and, on average, is about 0.2%, which is satisfactory. Indeed, in the high-retention domain, a 1% error in the determination of ν with $\nu \approx -0.2$ results in only a 0.25% error in the FFF parameter λ determined from retention data. Accordingly, the error in λ resulting from the use of Eq. 22 instead of the exact ν value will be at most about 0.1%, which is negligible in comparison with the experimental uncertainty in the measurement of the retention factor R. This error in λ will be smaller for smaller $|\nu|$ values. The numerical values of the a_i coefficients determined for the twelve solvents investigated are reported in Table 2 with ΔT and T_c expressed in °C (note that if T_c and ΔT were expressed in K instead of °C, the numerical values of a_2, a_4 and a_6 would be changed, but the value of ν would be unaffected).

It is instructive to evaluate the susceptibility of ν to small variations in the experimental conditions. In the case of ethylbenzene with $\Delta T = 60$°C and $T_c = 20$°C, one finds $d \ln |\nu| / d \ln \Delta T = 0.79$ and $d \ln |\nu| / d \ln T_c = -1.72$ (with T_c expressed in K). Accordingly, 1°C variations in ΔT and T_c induce 1.3% and 0.6% variations in ν, respectively. These variations, which are larger than typical temperature fluctuations observed experimentally, will therefore have a negligible influence on the determination of λ in thermal FFF, as far as the velocity profile is concerned (of course, these variations, especially the variation of ΔT, will directly influence the concentration profile and, hence, the retention factor, but this effect is not considered in the present study).

The correctness of the a_i coefficients reported in Table 2 lies on the accuracy of the experimental physico-chemical parameters of the solvent which influence the velocity profile. The most important one is the parameter B entering the viscosity Eq. 4. In the case of ethylbenzene with $\Delta T = 60$°C and $T_c = 20$°C, one finds $d \ln |\nu| / d \ln B = 0.91$. Therefore, a 1% variation of B (i.e. $\delta B = 11$ K for ethylbenzene) leads to a 0.9% variation in ν. In practice, the B parameter obtained by fitting experimental viscosity data according to Eq. 4 may not be rigorously equal to the true B parameter of the solvent investigated owing to the experimental uncertainty in the basic viscosity data, or Eq. 4 may not fit correctly the viscosity data in the whole temperature domain, in spite of its theoretical foundation. This source of error is probably the most important although its significance cannot easily be estimated. Nevertheless, the relatively high value of the correlation coefficient (generally larger than 0.999) obtained when fitting experimental data according to Eq. 4 gives confidence in the accuracy of the B parameter and of the resulting a_i coefficients in Eq. 22.

The influence of B on ν is shown in Fig. 5 for $T_c = 20$°C and two ΔT values (50 and 100°C). In the B range spanned by the twelve investigated

Table 2
Values of the a_i parameters entering the ν vs. ΔT and T_c relationship, $\nu = (a_1 T_c + a_2)\,\Delta T + (a_3 T_c + a_4)\,\Delta T^2 + (a_5 T_c + a_6)\,\Delta T^3$, with ΔT and T_c in °C

Solvent	a_1	a_2	a_3	a_4	a_5	a_6
Benzene	$3.2890 \cdot 10^{-5}$	$-5.7476 \cdot 10^{-3}$	$-2.3355 \cdot 10^{-7}$	$2.7828 \cdot 10^{-5}$	$7.9610 \cdot 10^{-10}$	$-7.7659 \cdot 10^{-8}$
2-Butanone	$2.4391 \cdot 10^{-5}$	$-4.2698 \cdot 10^{-3}$	$-1.4870 \cdot 10^{-7}$	$1.8096 \cdot 10^{-5}$	$4.5769 \cdot 10^{-10}$	$-4.6985 \cdot 10^{-8}$
Carbon tetrachloride	$3.1100 \cdot 10^{-5}$	$-5.4295 \cdot 10^{-3}$	$-2.1386 \cdot 10^{-7}$	$2.5182 \cdot 10^{-5}$	$7.0947 \cdot 10^{-10}$	$-6.9182 \cdot 10^{-8}$
Cyclohexane	$3.7850 \cdot 10^{-5}$	$-6.6216 \cdot 10^{-3}$	$-2.8678 \cdot 10^{-7}$	$3.3675 \cdot 10^{-5}$	$9.9830 \cdot 10^{-10}$	$-9.7197 \cdot 10^{-8}$
Cyclohexanone	$4.4449 \cdot 10^{-5}$	$-7.8087 \cdot 10^{-3}$	$-3.6313 \cdot 10^{-7}$	$4.3010 \cdot 10^{-5}$	$1.2979 \cdot 10^{-9}$	$-1.2948 \cdot 10^{-7}$
p-Dioxane	$3.2829 \cdot 10^{-5}$	$-5.7365 \cdot 10^{-3}$	$-2.3105 \cdot 10^{-7}$	$2.7502 \cdot 10^{-5}$	$7.6947 \cdot 10^{-10}$	$-7.7352 \cdot 10^{-8}$
Ethyl acetate	$2.6196 \cdot 10^{-5}$	$-4.5583 \cdot 10^{-3}$	$-1.6611 \cdot 10^{-7}$	$1.9285 \cdot 10^{-5}$	$5.2939 \cdot 10^{-10}$	$-5.0727 \cdot 10^{-8}$
Ethylbenzene	$2.7579 \cdot 10^{-5}$	$-4.7923 \cdot 10^{-3}$	$-1.8286 \cdot 10^{-7}$	$2.1212 \cdot 10^{-5}$	$6.1322 \cdot 10^{-10}$	$-5.6833 \cdot 10^{-8}$
Tetrahydrofuran	$2.3140 \cdot 10^{-5}$	$-4.0363 \cdot 10^{-3}$	$-1.3965 \cdot 10^{-7}$	$1.6848 \cdot 10^{-5}$	$4.3405 \cdot 10^{-10}$	$-4.2795 \cdot 10^{-8}$
Toluene	$2.7169 \cdot 10^{-5}$	$-4.7429 \cdot 10^{-3}$	$-1.7549 \cdot 10^{-7}$	$2.0883 \cdot 10^{-5}$	$5.6398 \cdot 10^{-10}$	$-5.5386 \cdot 10^{-8}$
o-xylene	$3.1016 \cdot 10^{-5}$	$-5.2335 \cdot 10^{-3}$	$-2.0980 \cdot 10^{-7}$	$2.3803 \cdot 10^{-5}$	$6.9511 \cdot 10^{-10}$	$-6.4920 \cdot 10^{-8}$
p-xylene	$2.6337 \cdot 10^{-5}$	$-4.5996 \cdot 10^{-3}$	$-1.6614 \cdot 10^{-7}$	$1.9918 \cdot 10^{-5}$	$5.1909 \cdot 10^{-10}$	$-5.2239 \cdot 10^{-8}$

solvents (from about 900 to 1800 K), ν is seen to vary approximately linearly, although their intercepts are not equal to 0 as they should be since a hypothetical $B = 0$ solvent would have a constant viscosity at all temperatures. Nevertheless, as organic solvents have B values lying within the range covered in Fig. 5, this near-linearity property can be used to obtain a rough estimate of the ν value for a solvent not listed in Table 1 but for which B is known. However, one cannot expect to obtain precise estimates as the temperature dependence of the thermal conductivity differs from one solvent to another, as reflected by the slight fluctuations of the data points in Fig. 5 around the regression line.

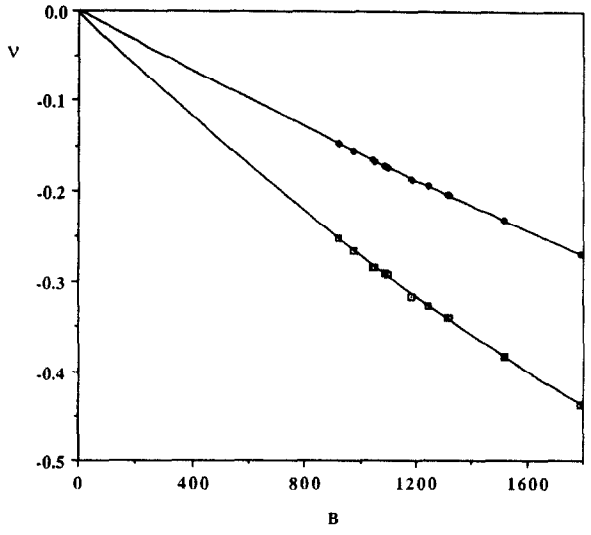

Fig. 5. Variations of the ν parameter with the solvent B constant. Upper curve, $\Delta T = 50$°C; lower curve, $\Delta T = 100$°C. $T_c = 20$°C.

The major interest in the calculation of ν according to Eq. 22 in connection with the data in Table 2 is that it allows one to take into account, with fair accuracy, the effect that deviations in the velocity profile have on calculations of the retention factor. Indeed, the calculation of the retention factor, R, of a polystyrene sample with molecular mass 300 000 using the exact velocity profile of the ethylbenzene carrier with $\Delta T = 60$°C and $T_c = 20$°C gives a value of 0.195. If the velocity profile was assumed to be parabolic, the error in R would be 19.5%, whereas using the third-degree polynomial velocity profile with the ν value estimated as indicated above as −0.200, the error in R is only 0.25%. The error in R appears in this instance to be reduced nearly by two orders of magnitude when taking into account the deviation of the

velocity profile from the parabolic shape by means of the third-degree profile.

5. Conclusions

Thermal FFF is mainly used to obtain information on the thermal diffusion properties and the molecular mass or size of a sample. The first step in this direction is to determine the basic FFF parameter λ from retention data. In order to take into account the deviation of the velocity profile from the ideal parabolic shape due to the temperature dependence of the viscosity, one suggests first calculating the ν parameter of the third-degree polynomial velocity profile to approximate the exact velocity profile by means of Eq. 22 and Table 2, for the actual operating conditions (solvent, ΔT, T_c). Then the basic FFF parameter λ can be obtained from the retention factor R using Eq. 17 for that calculated value of ν. Solving Eq. 17 for λ when R and ν are known can be done numerically using a classical iterative methods such as Newton's method or, most conveniently, by listing R values for as close as desired λ values with various spreadsheet applications, such as Excel, on microcomputers.

This study was motivated by the need for a practical method to take into account retention perturbations in thermal FFF arising from deviations of the velocity profile from the ideal parabolic shape due to the temperature dependence of the relevant parameters. It has been pointed out that, similarly, retention perturbations may also arise from deviations of the concentration profile from the ideal exponential shape [8]. Although the latter perturbations might be of the same order as the former and that the assumption of an exponential concentration profile made for obtaining Eq. 17 is not rigorously correct, Eq. 17 still serves as a very useful basis for taking into account the effect of the concentration profile distortion on retention. Work is in progress in this direction and will be presented in a forthcoming publication [16].

Acknowledgement

The assistance of Charles Van Batten in the determination of some of the coefficients in Table 2 is gratefully acknowledged.

References

[1] J.C. Giddings, *Science*, 260 (1993) 1456–1465.
[2] M. Martin and P.S. Williams, in F. Dondi and G. Guiochon (Editors), *Theoretical Advancement in Chromatography and Related Separation Techniques (NATO ASI Series: Mathematical and Physical Sciences*, Vol. 383), Kluwer, Dordrecht, 1992, pp. 513–580.
[3] T. Takahashi and W.N. Gill, *Chem. Eng. Commun.*, 5 (1980) 367–385.
[4] J. Janča, M. Hoyos and M. Martin, *Chromatographia*, 33 (1992) 284–286.
[5] M.N. Myers, K.D. Caldwell and J.C. Giddings, *Sep. Sci.*, 9 (1974) 47–70.
[6] G. Westermann-Clark, *Sep. Sci. Technol.*, 13 (1978) 819–822.
[7] S.L. Brimhall, M.N. Myers, K.D. Caldwell and J.C. Giddings, *J. Polym. Sci., Polym. Phys. Ed.*, 23 (1985) 2443–2456.
[8] J.C. Giddings, K.D. Caldwell and M.N. Myers, *Macromolecules*, 9 (1976) 106–112.
[9] J.J. Gunderson, K.D. Caldwell and J.C. Giddings, *Sep. Sci. Technol.*, 19 (1984) 667–683.
[10] M. Martin and J.C. Giddings, *J. Phys. Chem.*, 85 (1981) 727–733.
[11] G. Liu and J.C. Giddings, *Chromatographia*, 34 (1992) 483–492.
[12] M. Martin, M.N. Myers and J.C. Giddings, *J. Liq. Chromatogr.*, 2 (1979) 147–164.
[13] J.C. Giddings, M. Martin and M.N. Myers, *Sep. Sci. Technol.*, 14 (1979) 611–643.
[14] M. Martin and R. Reynaud, *Anal. Chem.*, 52 (1980) 2293–2298.
[15] M.E. Schimpf, P.S. Williams and J.C. Giddings, *J. Appl. Polym. Sci.*, 37 (1989) 2059–2076.
[16] M. Martin, J. Belgaied, C. Van Batten and M. Hoyos, in preparation.
[17] K.D. Caldwell, M. Martin and J.C. Giddings, unpublished results.
[18] R.B. Bird, W.E. Stewart and E.N. Lightfoot, *Transport Phenomena*, Wiley, New York, 1960, Ch. 3.
[19] A.B. Shah, J.F.G. Reis, E.N. Lightfoot and R.E. Moore, *Sep. Sci. Technol.*, 14 (1979) 475–497.
[20] R.C. Reid, J.M. Prausnitz and B.E. Poling, *The Properties of Gases and Liquids*, McGraw-Hill, New York, 4th ed., 1987, Ch. 9.

[21] E. Guyon, J.-P. Hulin and L. Petit, *Hydrodynamique Physique*, InterEditions et Editions du CNRS, Paris and Meudon, 1991, Ch. 2.
[22] R.B. Bird, W.E. Stewart and E.N. Lightfoot, *Transport Phenomena*, Wiley, New York, 1960, Ch. 8.
[23] R.C. Reid, J.M. Prausnitz and B.E. Poling, *The Properties of Gases and Liquids*, McGraw-Hill, New York, 4th ed., 1987, Ch. 10.
[24] H.-G. Elias, in J. Brandrup and E.H. Immergut (Editors), *Polymer Handbook*, Wiley, New York, 2nd ed., 1975, Ch. 7.
[25] J.C. Giddings, L.K. Smith and M.N. Myers, *Anal. Chem.*, 47 (1975) 2389–2394.
[26] S.L. Brimhall, M.N. Myers, K.D. Caldwell and J.C. Giddings, *Sep. Sci. Technol.*, 16 (1981) 671–689.